Measurement of Wake Vortex Strength by Means of Acoustic Back Scattering

David C. Burnham,* Thomas E. Sullivan,†
U. S. Department of Transportation, Transportation Systems Center, Cambridge, Mass.

and

Leonard S. Wilk‡
MIT, Measurement Systems Laboratory, Cambridge, Mass.

A simple acoustic sounder is shown to produce reliable velocity profiles of aircraft wakes at altitudes below 50 m. Data collection during normal airport landing operations was feasible because the sensor does not intrude into the airspace being measured. A spatial scan through the wake is obtained when the ambient wind transports the wake through the sounder beam. The characteristics of the scattered signals and their spectral densities are presented as intensity modulated CRT displays termed "Acoustograms." The data are processed to yield the radial dependence of the velocity and circulation in the wake vortices. The circulation data are fitted to a simple model with two parameters: strength and core radius. The spatial and velocity resolution of the sounder is adequate to measure vortex strength but not to probe details of the core structure. Reliable measurements using this technique are possible only when the vortex transport velocity is well-defined.

I. Introduction

ACOUSTIC back scattering is a well-established[1] technique for studying the properties and motions of the atmosphere. This paper describes a study of aircraft wake vortices using an acoustic sounder similar to those used in meteorological studies.[2] The first experiments in the fall of 1972 were designed as a simple test to determine whether wake vortices could be detected by acoustic back scattering. A tracking system based on this concept was recently reported.[3] The major accomplishment of the work presented here is the discovery that a simple acoustic sounder is in fact a powerful tool for measuring the strength of aircraft wake vortices. Currently, an array of sounders is being used to study vortex decay at Kennedy International Airport.

After the first sounder data had been collected, considerable effort was expended in devising suitable methods of displaying the data for evaluation and comparison. Subsequently, methods were developed for extracting vortex information from the data. The purpose of this paper is to describe these methods and to present the capabilities and limitations of the "vortex sounder" as a remote sensing technique.

II. Characteristics of the Vortex Sounder

The acoustic sounder used in this study (shown in Figure 1) is similar to those used in meteorological studies,[2] but it has some unique features because of the short range and high resolution required for wake vortex sensing. A conventional acoustic sounder radiates a pulse of energy into a narrow vertical beam. The energy scattered back from the atmosphere is detected and analyzed for Doppler shifts. The range y of the scattering is determined from the time delay t after transmission and the speed of sound c by the relationship $y=ct/2$. For vertical beam orientation the Doppler shift depends only upon the vertical component w of the wind velocity v in the scattering volume determined by the range gate and the antenna beam(s). The sounder is therefore relatively insensitive to the ambient wind which is predominantly horizontal. Consequently, the observed Doppler shifts directly characterize the velocity distribution in the aircraft vortices being studied.

In the tests reported here the aircraft vortices were located near the ground. A maximum range of 50 m (300-m/sec pulse repetition period) and a range resolution of 3.3 m (20-msec pulse length) were selected for most of the measurements. For 180° scattering the Doppler calibration is $w=c(\Delta f/2f)$ where f is the transmitted frequency and Δf is the mean frequency shift in the power spectral density of the scattered signal. In order to minimize the frequency spread in the Doppler spectra a smooth modulation envelope is used for the transmitted signal. For a smooth 20-msec (full-width at half-maximum voltage) pulse the 3-dB frequency width is roughly 35 Hz, corresponding to a velocity width of 1.7 m/sec for the typical frequency of 3.5 kHz used in the tests. The Doppler spectra are processed with a real-time spectrum analyzer (Federal Scientific Model UA-15A) with a response width (power) of 18 msec, a 3-dB Doppler width of 30 Hz, and a resolution of 20 Hz. As shown later in Fig. 4, the analyzed power spectra have a minimum rms frequency deviation from the mean of about 25 Hz (1.2 m/sec at 3.5 kHz). In the absence of wake vortices, the observed standard deviation of the mean frequency Δf was typically less than 12 Hz (0.6 m/sec at 3.5 kHz).

The primary difference between the vortex sounder and conventional meteorological sounders is the use of separate adjacent antennas for transmitting and receiving. This configuration was selected to assure that vortex returns could be monitored very close to the ground. Separating the receiver from the transmitter eliminates ringing which could obscure the return signal for perhaps 150 msec (25-m height) in a single antenna system. As shown in Figure 1, the beams from the two antennas are oriented to intersect about 20 m above the ground. Diffraction of the two beams results in satisfactory beam overlap at higher altitudes. The sounder antennas are 1.2-m paraboloidal dishes of 0.76-m focal length fed by a conical horn and 60-W (electrical) driver. The beam width at 3.5-KHz frequency is estimated to be 7° for this dish which is 12 wavelengths in diameter with −10-dB edge illumination.

Received Aug. 11, 1975; revision received March 4, 1976. The authors wish to thank R.D. Kodis for his suggestions.

Index categories: Satety; Aircraft Landing Dynamics; Jets, Wakes, and Viscid-Inviscid Flow Interactions.

*Staff Scientist.

†Staff Engineer.

‡Associate Director for Engineering Development. Now at C.S. Draper Laboratory, Inc.

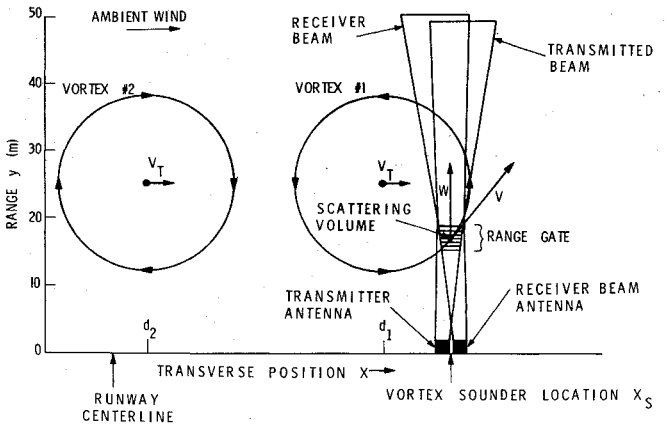

Fig. 1 Geometry of the vortex sounder (not to scale). V_T is the transport velocity of the vortex.

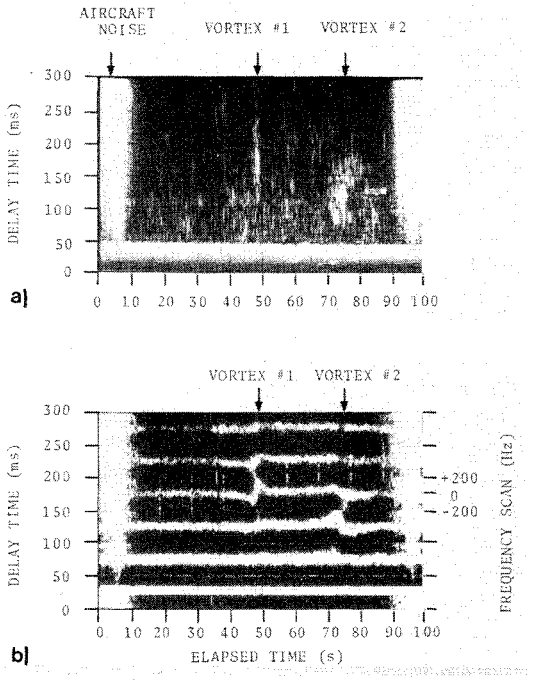

Fig. 2 Acoustic scattering data for the vortices from a B-707 aircraft in landing configuration. November 13, 1973. a) Basic acoustogram. b) Spectral acoustogram: 6 range gates with a Doppler frequency scan of 400 Hz.

Because the intensity of the scattered signals is small, care must be taken to exclude extraneous acoustic and electrical noise. Sources of ambient noise and ground clutter are generally located at ground level in the side-lobe response of the antennas. A plywood baffle extending 1.2 m above the dish is placed around the antennas to attenuate the side lobes. The inside of the baffle is covered with convoluted polyfoam to reduce reflections. Electrical noise is suppressed by locating a low-noise preamplifier close to the receiver transducer.

The received signals are suitably conditioned before they are recorded for processing. First, the signals pass through a high-pass filter to eliminate the predominantly low-frequency ambient noise and then through a low-Q band-pass filter to isolate the transmitted frequency. The signal gain is then increased linearly[2] with time t in order to compensate for the expected range ($y=ct/2$) dependence of the signal amplitude. Scattering from a uniform distribution of scatterers gives an inverse square range dependence (y^{-2}) for the scattered signal power (y^{-1} for signal amplitude) under the assumption of complete beam overlap.

III. Characteristics of Vortex Back Scattering

The evaluation of vortex scattering data is simplified by a convenient means of displaying multidimensional data. In this section the vortex signals are shown as intensity modulated oscilloscope pictures, termed "acoustograms." In the basic acoustogram [see Fig. 2a] the oscilloscope brightness indicates the amplitude of the acoustic return signal as a function of time. The scan format of the picture is a fast scan (time t) in the vertical direction indicating range ($y=ct/2$) and a slow scan in the horizontal direction indicating elapsed time T. When an aircraft vortex passes through the vertical acoustic beam the resulting acoustogram gives a picture of the scattering cross section as a function of location within the vortex under the assumption that the properties of the vortex are unchanged during the transit time. Although the linear time variable gain cancels out the normal range dependence of the scattered signals, some range distortion of the signal amplitude is produced by reduced beam overlap at low altitudes and by acoustic attenuation at high altitudes.

A number of salient features may be noted in the acoustogram of Fig. 2a. The constant bright band across the bottom is the direct reception of the transmitted pulse. The bright vertical patch at the left is the noise generated by the arriving aircraft and that on the right is the noise of the next aircraft. The increasing width of these patches toward the top of the acoustogram is caused by the time variable gain. The scattered signals occurring before the arrival of the aircraft vortices are due to ambient atmospheric turbulence. The passage of the two aircraft vortices through the antenna beam is correlated with increased scattering. The vortex structure appears elliptical on the acoustogram because the effective horizontal distance scale ($x=V_TT$ where V_T is the transport speed of the vortex through the beam) differs from the vertical scale. The periodic series of dotted vertical lines across the center of the acoustogram (10-sec period) is caused by electromagnetic interference from an airport radar.

The Doppler shifts in the scattered signals can be displayed as a "spectral acoustogram," shown in Fig. 2b. In this display the vertical scan is broken into six range gates which are analyzed by the real-time spectrum analyzer. Within each range gate the spectrum is scanned in time to give a vertical readout of signal amplitude vs. frequency. Successive vertical scans produce horizontal bright lines plotting the Doppler shift for each range gate as a function of elapsed time. The passage of a vortex core through the antenna beam is signaled by a change in the sign of the Doppler shifts. The altitude of the vortex core is indicated by the range gate showing the largest Doppler shifts before and after the core passage. The pattern of Doppler shifts in Fig. 2b is that expected from the counter rotating pair of wake vortices (see Fig. 1). The ver-

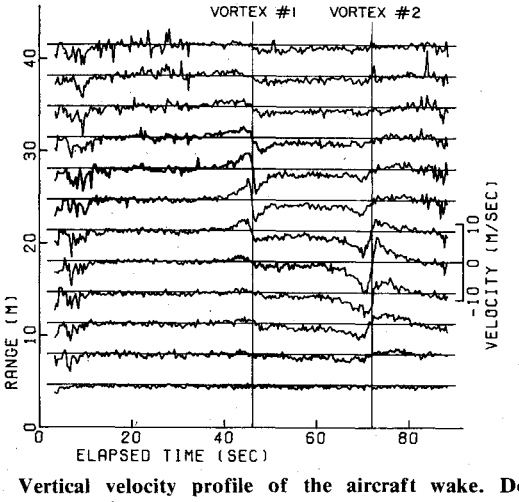

Fig. 3 Vertical velocity profile of the aircraft wake. Doppler frequency scan = 600 Hz.

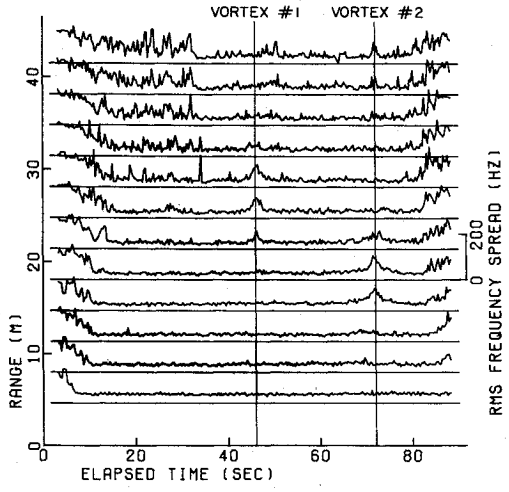

Fig. 4 RMS frequency spread of the vortex sounder data.

tical wind is down (positive Doppler shifts) between the two vortices and is up (negative Doppler shifts) outside the two vortex cores. The convenience of viewing all the Doppler data for one aircraft passage on a single spectral acoustogram was obtained at the expense of both range and velocity resolution. A total of 15 range resolution elements are actually available for a period of 300 msec and a pulsewidth of 20 msec. The limited dynamic response of the acoustogram intensity causes the Doppler peaks to be broadened.

Analysis of the data with full Doppler resolution was obtained both manually from an oscillograph display and by direct computer digitization of the spectrum analyzer output. Figure 3 shows a computerized version of the spectral acoustogram of Fig. 2, where the mean value of the Doppler spectrum is used to determine the vertical velocity distribution within the vortex. Figure 4 shows the rms frequency spread for the same run. The frequency spread gives an indication of the accuracy of the velocity measurement and becomes larger than its minimum value of 25 Hz when the noise is high, the signal is low, or the velocity changes rapidly within the resolution of the beam (e.g., at the vortex core). The frames containing radar interference have been eliminated from Figs. 3 and 4.

Before the observed vortex scattering can be discussed it is necessary to consider the possible scattering mechanisms listed in Table 1.

Incoherent scattering occurs from turbulence imbedded in the vortex and therefore has Doppler shifts characteristic of the vortex velocity field. The angular dependence[4] of such scattering depends upon the nature of the turbulence. The cross section for velocity fluctuation scattering vanishes at a scattering angle of 180°. Thus, apart from multiple scattering, only temperature fluctuations can contribute to incoherent back scattering. Early studies[5] of incoherent acoustic scattering from wake vortices avoided the back scatter geometry since temperature fluctuations were expected to be much weaker than velocity fluctuations. One would expect that the temperature fluctuations in an aircraft wake are strongly affected by entrained engine exhaust. One objective for the present study was to compare the vortex signals for aircraft with different engine locations.

Table 1 Scattering mechanisms

Incoherent	Coherent
1) Temperature fluctuations	3) Refraction
2) Velocity fluctuations	4) Diffraction
	5) Reflection

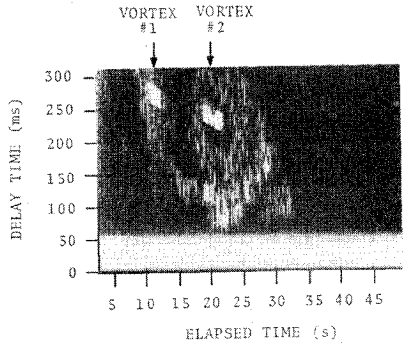

Fig. 5 Acoustic scattering data for the vortices from a B-707 aircraft in holding configuration, October 18, 1972. Note the sharp core reflections at 12 and 21 sec.

Coherent scattering occurs from the vortex as a whole and therefore exhibits Doppler shifts characteristic of the vortex transport velocity, rather than the vortex velocity field. These Doppler shifts can generally be ignored since vortex transport speeds are generally much smaller than the wind speeds within the vortex, especially for the vertical velocity component measured in this work. The dominant mechanism for coherent scattering depends upon the scale of the scattering disturbance relative to the acoustic wavelength. Refraction is the bending of a sound beam by variations in the acoustic propagation medium. Diffraction is the spreading of a beam which is proportional to the ratio of the acoustic wavelength to the spatial extent of the scatterer. For large wavelengths, the diffractive spreading can dominate the refractive bending. Reflection occurs when the medium changes significantly in a wavelength such that part of the sound is scattered in the backwards direction. The distinction between diffraction and reflection becomes meaningless for scatterers smaller than one wavelength. For aircraft vortices the predominant effect of refraction[6] is a rotation of the propagation vector by an angle which is unlikely to exceed 90°.[6,7] Thus, coherent scattering at 180° is probably due to diffraction/reflection, which can occur only if the vortex core is comparable in size to the acoustic wavelength.

The vortex sounder was first tested at the National Aviation Facilities Experimental Center (NAFEC) using a dedicated B-707 aircraft (See Fig. 5 for sample data). Subsequently, data were collected for a variety of aircraft landing at Kennedy International Airport. Sample data runs are shown in Figs. 1 and 6. The experimental observations can be summarized as follows:

1) Under the conditions of the tests sufficient scattering occurred to allow reliable measurement of the vortex velocity field for all commericial jet aircraft of the B-737, DC-9 class or larger. The scattering was weaker for aircraft with tail-mounted engines as expected, but it was nevertheless adequate for satisfactory measurements.

2) Vortices from aircraft types and configurations known to produce small vortex cores[8] often show a strong, sharp core reflection which has little Doppler shift. Such scattering behavior was observed for B-707 holding configuration vortices (NAFEC tests) and for B-727, B-737, DC-9 and DC-10 landing configuration vortices (Kennedy tests). The sharpness of the core reflection is especially evident in Fig. 5 where a square modulation envelope was transmitted. Occasionally, small core vortices also generate a whistling sound which shows up in an acoustogram as a narrow vertical noise streak.

3) Under some atmospheric conditions the region between two well-separated vortices produces surprisingly little scattering, as shown in Fig. 6. This effect is probably due to a strong decrease in ambient turbulence with altitude. The strong downdraft produced by the vortex pair fills the region between the vortices with less turbulent air from altitudes above the vortex system.

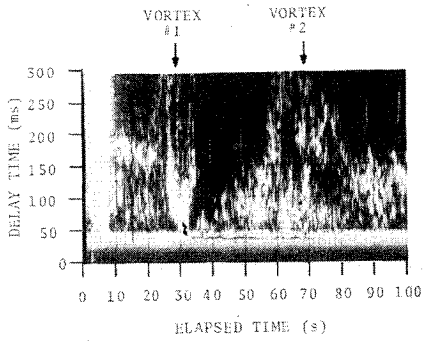

Fig. 6 Acoustic scattering data for the vortices from a B-747 aircraft in landing configuration, November 14, 1973.

IV. Measurements of Vortex Strength

In order to extract vortex information from the measured velocity field it is helpful to have a theoretical model for the vortex. For an axially symmetric vortex, the circulation is given by

$$\Gamma(r) = 2\pi r v(r) \tag{1}$$

where $v(r)$ is the vortex tangential velocity as a function of radius r. The vortex strength is defined as the asymptotic value Γ_∞ of the circulation for large radii where $v(r)$ varies inversely with r:

$$v(r) = \Gamma_\infty / 2\pi r \tag{2}$$

The data processing makes use of a two-parameter circulation model:

$$\Gamma(r) = \Gamma_\infty r^2 / (r^2 + r_c^2) \tag{3}$$

which is convenient for calculations and also gives a realistic representation of actual vortices. The core radius r_c represents both the radius of maximum velocity and the radius where

$$\Gamma(r_c) = \tfrac{1}{2}\Gamma_\infty$$

As illustrated in Fig. 1, the vortex sounder measures the vertical velocity profile in a plane through the vortex pair. The data analysis is simplified if one can relate the measurements to the expected vertical velocity field $w(x,y)$ of a single vortex, which takes the form

$$w(x,y,d,h) = v(r)\,[(x-d)/r] \tag{4}$$

where d is the vortex lateral position (x axis), h is the vortex height (y axis), and the vortex radius is given by

$$r = [(x-d)^2 + (y-h)^2]^{1/2}$$

For the vortex model in Eq. (3) the velocity field assumes the following simple form

$$w(x,y,d,h) = \Gamma_\infty (x-d) / [(x-d)^2 + (y-h)^2 + r_c^2] / 2\pi \tag{5}$$

Equations 4 and 5 must be modified when the vortex is near the ground. The boundary conditions at the ground ($y=0$) can be satisfied by adding an image vortex of opposite circulation at position d and height $-h$.

The expected single vortex velocity profile $W(X_s, Y, T)$ measured by a vortex sounder at location X_s is given by

$$W(X_s, y, T) = w[X_s, y, d(T), h(T)] \tag{6}$$

where the time dependence of the vortex position (d,h) is included explicitly. $W(X_s,y,T)$ is actually a spatial average of

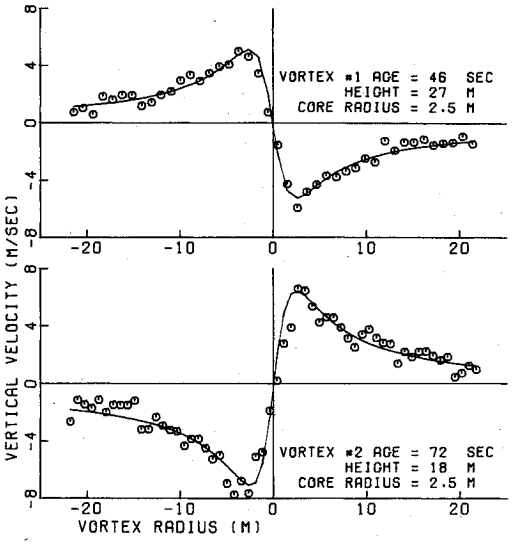

Fig. 7 Radial velocity profile of the two wake vortices. The points are experimental and the solid curve is given by a model.

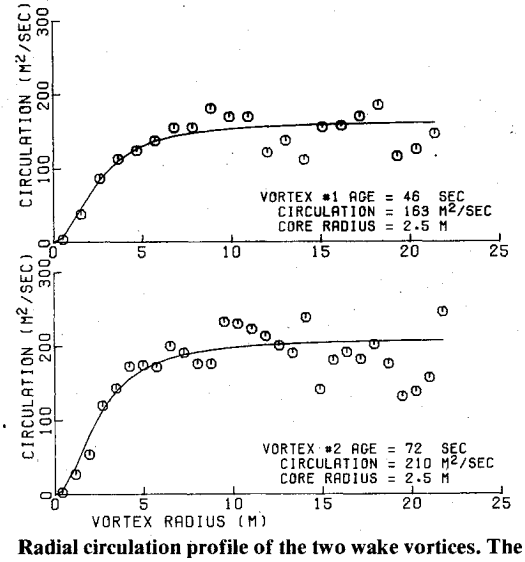

Fig. 8 Radial circulation profile of the two wake vortices. The points are experimental and the solid curve is the best fit to the model described in the text.

$w(x,y)$ over the sounder range (y) and beam or position (X_s) resolution. The transformation of the time-dependent W data to yield spatial vortex information is based on the assumption that the vortex moves horizontally at constant speed V_T, i.e. $h(T) =$ constant and $d(T) = X_s + TV_T$, where the time $T=0$ is defined by the vortex arrival over the sounder. Under these assumptions the measured velocity at range $y=h$ directly gives the vortex tangential velocity $v(r)$

$$W(X_s, h, T) = v(TV_T) \tag{7}$$

One should note that any error in V_T translates directly into an error in vortex radius and therefore, according to Eq. (1), a proportional error in circulation.

Two different ways of estimating V_T were used in analyzing the data. The simplest way is to assume a constant transport velocity from the point X_0 and time T_0 of vortex creation and use the observed arrival time T_s at the vortex sounder to give

$$V_T = (X_s - X_0) / (T_s - T_0) \tag{8}$$

This method is most reliable for strong cross winds where vortex induction effects on V_T are small and for large sensor

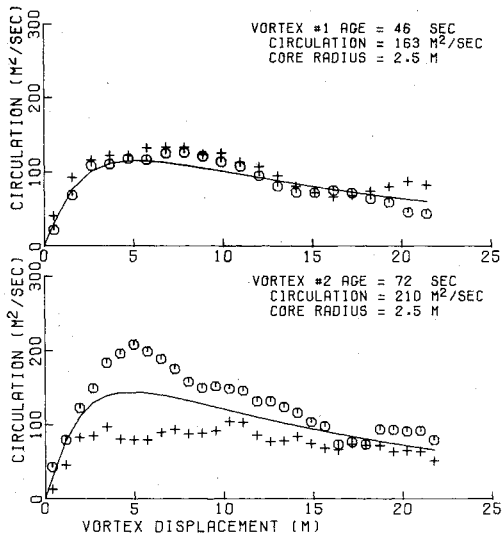

Fig. 9 Circulation line integral as a function of vortex displacement from the sounder location. The experimental data from before (after) the vortex arrival are plotted as circles (crosses) and have been smoothed by a three-point running average. The solid curve is given by a model.

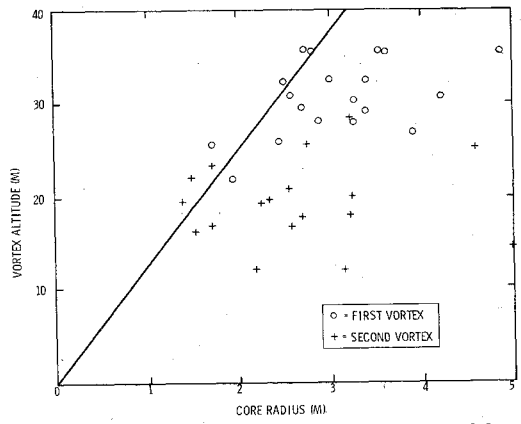

Fig. 10 Vortex altitude vs core radius. Data are plotted for vortices with circulation greater than 100 m^2/sec from a series of fifty runs

displacements where errors in initial vortex position X_0 are relatively unimportant. The second way of estimating V_T is to use the output from a vortex tracking system (e.g., an array of anemometers or vortex sounders). Observations of vortex tracks at the airport test location (700 m from runway threshold) suggested the following simple estimates for an effective initial position X_0 which gives a correct value for V_T from Eq. (8):

1) First vortex (downwind): $X_0 = 25$ m downwind from runway centerline.

2) Second vortex (upwind): $X_0 =$ runway centerline.

Figures 7 and 8 show the results of processing the velocity field data of Figure 3 by the techniques described in this section. The arrival time T_s and height h for each vortex was obtained by finding a maximum in the correlation of the velocity data with a function that is a single cycle square wave in the time dimension and a peaked function in range. Figure 7 displays the vortex tangential velocity [Eq. (7)] as a function of displacement from the vortex center. The velocity for height h is obtained by interpolation between adjacent range gates. The circulation for a given radius r is plotted in Fig. 8 as the average of the values from Eq. (1) for the velocities at $\pm r$ in Fig. 7. These circulation results are then independent of uniform offsets in the velocity measurements.

In order to characterize the vortex data in a convenient way the circulation data in Fig. 8 have been fitted to the two-parameter form of Eq. (3). The corresponding velocity curve is plotted in Fig. 7. The circulation fit was obtained by at least square method in which the points are weighted as velocity squared. This procedure accounts for the larger errors expected at low velocities. Theoretical [Eq. (2)] rather than experimental values of the velocity are used to avoid biasing the data.

In order to study slowly moving or stalled vortices where V_T is poorly defined, it would be desirable to measure vortex circulation from range data taken at a single time. In this case one must determine the four unknown parameters Γ_∞, h, d, and r_c of Eqs. (2) – (6) from the vertical velocities at 10 to 20 range gates. In pursuing this goal, it was found that the line integral of the vortex velocity along the sounder beam is a convenient indicator of circulation. It can be simply evaluated from the sum of all range gate velocities and should yield half the total circulation Γ_∞ under the conditions $r_c << d << h$. Figure 9 plots twice the sounder line integral as a function of vortex displacement d for the data of Fig 3. The solid lines in Fig. 9 are calculated from the measured values Γ_∞, h and r_c, including the effects of the image vortex. For fresh vortices (e.g. vortex #1 in Fig. 9) the observed line integrals are in reasonable agreement with the calculated values. For old vortices (e.g. vortex #2 in Fig. 9) the velocity field becomes distorted and the agreement is poor. The value of circulation obtained from the line integral must be corrected for d, h, and r_c to yield an accurate estimate for Γ_∞. For $d < h$ the range with maximum velocity gives an accurate indication of vortex height. For $d > r_c$ the core radius has little effect on the results. A number of data parameters were evaluated for estimating d in the range $r_c < d < h$. The best estimates of d were inaccurate even for fresh vortices and gave valid results only for $d < h/2$. One must conclude that single time measurements of vortex strength are likely to be unreliable, especially for old vortices. Thus, it appears to be impractical to extract reliable vortex strength data unless V_T is well defined. Consequently, stalled vortices cannot be measured by this technique. However, if two adjacent vortex sounders were combined with a ground level anemometer array in between it is probably feasible to measure vortex circulation directly as a line integral.

An indication of the spatial resolution of the system is given in Fig. 10 which shows the core radius as a function of vortex height for a series of data runs. The measured core radius gives a reasonable estimate of the actual core radius if it is significantly larger than the limiting value indicated by the solid line [$r_c = \alpha h$ with $\alpha = 0.08$ rad (4.5°)].

The data processing techniques described here are particularly suited for vortices which have had time to separate and become distinct. The results can be distorted by vortex overlap for larger cross winds or smaller displacements X_s of the sounder from the runway centerline ($X_s = 180$ m here).

V. Conclusion

The vortex sounder described in this paper provides an inexpensive nonintrusive method of probing the velocity fields of aircraft wake vortices with moderate spatial and velocity resolution. Although the vortex sounder has insufficient resolution to probe the vortex core, it is well-suited for measuring vortex strength which depends upon the slowly varying velocity field away from the core. Measurements of vortex circulation are of particular interest because the hazard to other aircraft is related to vortex strength. For this purpose the vortex sounder offers a number of advantages over instrumented towers[9] which have provided the most detailed information about wake vortex velocities. Unfortunately, towers require the use of dedicated aircraft for safety and may also distort the vortex flow and affect its decay. Because the sounder does not intrude into the space being probed, it presents no hazard to the generating aircraft and does not disturb the vortices. Currently TSC is taking advantage of this feature to study the decay of wake vortices at Kennedy Air-

port during normal landing operations. An array of sounders is used to measure the strength of the same vortex at different ages. A final advantage of the vortex sounder over most instrumented tower measurements is the absence of response to the horizontal ambient wind. The hot-wire anemometers normally used on towers respond simultaneously to horizontal and vertical velocities so that unambiguous separation of the vortex velocity field and the ambient wind is difficult.

References

[1]Beran, D.W., Willmarth, B.C., Carsey, F.C., and Hall, F.F., "An Acoustic Doppler Wind Measuring System," *Journal of the Acoustical Society of America,* Vol. 55, No. 2, Feb. 1974, pp. 334-338.

[2]Beran, D.W., Little, C.G., and Willmarth, B.C., "Acoustic Doppler Measurements of Vertical Velocities in the Atmosphere," *Nature,* Vol. 230, No. 5290, Mar. 19, 1971, pp. 160-162.

[3]Balser, M., McNary, C.A., and Nagy, A.E., "Acoustic Back Scatter Radar System for Tracking Aircraft Trailing Vortices," *Journal of Aircraft,* Vol. 11, Sept. 1974, pp. 556-562.

[4]Little, C.G., "Acoustic Methods for the Remote Probing of the Lower Atmosphere," *Proceedings of the IEEE,* Vol. 57, No. 4, April 1969, pp. 571-578.

[5]Balser, M., Nagy, A., and McNary, C., "Acoustic Analysis of Aircraft Vortex Characteristics," Federal Aviation Administration, U.S. Department of Transportation, Rept. No. FAA-RD-72-81, July 1972.

[6]Georges, T.M., "Acoustic Ray Paths through a Model Vortex with a Viscous Core," *Journal of the Acoustical Society of America,* Vol. 51, Pt. 2, Jan. 1972, pp. 206-209.

[7]Burnham, D., Kodis, R., and Sullivan, T., "Observations of Acoustic Ray Deflection by Aircraft Wake Vortices." *Journal of the Acoustic Society of America,* Vol. 52, Pt. 2, July 1972, pp. 431-433.

[8]Burnham, D.C., and Sullivan, T.E., "Influence of Flaps and Engines on Aircraft Wake Vortices." *Journal of Aircraft,* Vol. 11, Sept. 1974, pp. 591-592.

[9]Garodz, L.J., "Measurements of Boeing 747, Lockheed C5A and other Aircraft Vortex Wake Characteristics by Tower Fly-By Technique," *Aircraft Wake Turbulence and Its Detection,* edited by J.H. Olsen, A. Goldburg, and M. Rogers, Plenum Press, New York, 1971, pp. 265-285.